Observations of $^{14}CO_2$ in ecosystem respiration from a temperate deciduous forest in Northern Wisconsin

RESEARCH ARTICLE

Key Points:
- We measured the radiocarbon composition of forest ecosystem respiration
- Two atmospheric approaches gave an average respired C age of 1–19 years
- This study provided observational constraints for the CASA earth system model

Observations of $^{14}CO_2$ in ecosystem respiration from a temperate deciduous forest in Northern Wisconsin

Claire L. Phillips[1], Karis J. McFarlane[2], Brian LaFranchi[2,3], Ankur R. Desai[4], John B. Miller[5,6], and Scott J. Lehman[7]

[1]Department of Crops and Soil Science, Oregon State University, Corvallis, Oregon, USA, [2]Center for Accelerator Mass Spectrometry, Lawrence Livermore National Laboratory, Livermore, California, USA, [3]Now at Combustion Research Facility, Sandia National Laboratory, Livermore, California, USA, [4]Department of Atmospheric and Oceanic Sciences, University of Wisconsin, Madison, Wisconsin, USA, [5]Global Monitoring Division, NOAA Earth System Research Laboratory, Boulder, Colorado, USA, [6]CIRES, University of Colorado Boulder, Boulder, Colorado, USA, [7]INSTAAR, University of Colorado Boulder, Boulder, Colorado, USA

Abstract The $^{14}CO_2$ composition of plant and soil respiration can be used to determine the residence time of photosynthetically fixed carbon before it is released back to the atmosphere. To estimate the residence time of actively cycled carbon in a temperate forest, we employed two approaches for estimating the $\Delta^{14}CO_2$ of ecosystem respiration ($\Delta^{14}C\text{-}R_{eco}$) at the Willow Creek AmeriFlux site in Northern Wisconsin, USA. Our first approach was to construct nighttime Keeling plots from subcanopy profiles of $\Delta^{14}CO_2$ and CO_2, providing estimates of $\Delta^{14}C\text{-}R_{eco}$ of 121.7‰ in June and 42.0‰ in August 2012. These measurements are likely dominated by soil fluxes due to proximity to the ground level. Our second approach utilized samples taken over 20 months within the forest canopy and from 396 m above ground level at the nearby LEF NOAA tall tower site (Park Falls, WI). In this canopy-minus-background approach we employed a mixing model described by Miller and Tans (2003) for estimating isotopic sources by subtracting time-varying background conditions. For the period from May 2011 to December 2012 the estimated $\Delta^{14}C\text{-}R_{eco}$ using the Miller-Tans model was 76.8‰. Together, these $\Delta^{14}C\text{-}R_{eco}$ values represent mean R_{eco} carbon ages of approximately 1–19 years. We also found that heterotrophic soil-respired $\Delta^{14}C$ at Willow Creek was 5–38‰ higher (i.e., 1–10 years older) than predicted by the Carnegie-Ames-Stanford Approach global biosphere carbon model for the 1×1 pixel nearest to the site. This study provides much needed observational constraints of ecosystem carbon residence times, which are a major source of uncertainty in terrestrial carbon cycle models.

1. Introduction

The future rate of increase in atmospheric CO_2 concentrations will depend not only on anthropogenic emissions from combustion of fossil fuels and land use change but also on the turnover time of carbon in terrestrial ecosystems [*Carvalhais et al.*, 2014; *Friend et al.*, 2014]. Carbon turnover time in plants and soils is a critical and highly uncertain variable regulating climate-carbon feedbacks. Radiocarbon (^{14}C) is an excellent tool for determining the mean age and turnover time of carbon in terrestrial pools, as demonstrated by studies of soils [*Gaudinski et al.*, 2000; *Trumbore*, 2000], plants [*Gaudinski et al.*, 2009; *Richardson et al.*, 2013], and aquatic systems [*Neff et al.*, 2006]. There is a large spread in the turnover time of terrestrial carbon pools, however, and estimating turnover at larger spatial scales has relied on model integration with uncertainties regarding the number, size, and turnover times of different carbon pools. The goal of this study was to evaluate two different methods that make use of atmospheric observations in order to provide estimates of $\Delta^{14}CO_2$ of ecosystem respiration ($\Delta^{14}C\text{-}R_{eco}$) and to infer carbon residence times at the Willow Creek AmeriFlux Site in Northern Wisconsin (US-WCR, hereafter WCR).

The utility of radiocarbon for estimating carbon turnover stems from (1) the fact that ^{14}C abundance in an isolated sample decreases quantitatively through time as a result of radioactive decay (this is relevant, however, only for carbon pools with very long persistence, as the half-life of ^{14}C is 5730 years), (2) the presence of excess "bomb" $^{14}CO_2$ in the atmosphere, which is a legacy of thermonuclear weapons testing in the 1950s and 1960s, and (3) the continued decline in atmospheric $\Delta^{14}C$, which has resulted from assimilation of excess "bomb" ^{14}C by oceanic and terrestrial reservoirs and from emissions of ^{14}C-free CO_2 from fossil fuel combustion. Levels of

atmospheric $\Delta^{14}CO_2$ peaked in the early 1960s and have been gradually declining since the 1963 Limited Test Ban Treaty, which prohibited aboveground weapons testing. Based on the rate of atmospheric $\Delta^{14}CO_2$ decline and models of ocean and terrestrial exchange, the mean global turnover time of terrestrial carbon has been estimated between 10 and 35 years [*Graven et al.*, 2012; *Naegler and Levin*, 2006]. Additionally, using observation-based global estimates of terrestrial carbon stocks and gross primary productivity, *Carvalhais et al.* [2014] estimated mean global carbon turnover time as 23 years (95% CI = 19–30 years).

The residual bomb carbon signal can also be measured directly in soils and trees, and measurement of these materials has been used to infer a very large range in residence times among related carbon reservoirs. For example, the mean age of C in leaf buds and new roots in a northern hardwood forest was estimated at 0.7 years [*Gaudinski et al.*, 2009], but long-lived tree roots had a much larger estimated age of 8–13 years [*Gaudinski et al.*, 2010]. Stem wood starch and sugars at three forest sites in the northeastern United States has a mean carbon age of 7–14 years [*Richardson et al.*, 2013]. Residence times for soil carbon can range from years to millennia, depending on numerous factors including but not limited to the following: depth [*Trumbore*, 2000], mineral associations [*Heckman et al.*, 2014; *Torn et al.*, 1996], and ecosystem-specific plant-microbial-environment interactions [*Schmidt et al.*, 2011]. The heterogeneity of terrestrial carbon reservoirs makes it inherently difficult to reconcile fine-scale measurements with global-scale estimates of terrestrial residence times. Ideally, we would like to be able to determine carbon residence times at the ecosystem scale—coarse enough to integrate plant and soil reservoirs but fine enough to assess the influence of specific vegetation types and climate regimes.

Due to roughly decadal carbon storage in plant and most soil pools, $\Delta^{14}C\text{-}R_{eco}$ is expected to be relatively enriched in ^{14}C with respect to that in the contemporary atmosphere. The isotopic disequilibrium between $\Delta^{14}CO_2$ taken up through photosynthesis and released by respiration is an important variable that has been used to develop top-down estimates of biospheric CO_2 exchange from global trends in atmospheric $\Delta^{14}CO_2$. The ^{14}C isotopic disequilibrium has been inferred from various terrestrial carbon cycle models, ranging from simple models with only a single terrestrial carbon pool [e.g., *Graven et al.*, 2012; *Naegler and Levin*, 2006], to the mechanistic, multiple-pool CASA carbon model (Carnegie-Ames-Stanford Approach) [*Thompson and Randerson*, 1999], applied for $^{14}C/^{12}C$ predictions by *Miller et al.* [2012]. Direct field measurements of respired $\Delta^{14}CO_2$ from terrestrial ecosystems are few, however, and have focused primarily on soil respiration [*Czimczik et al.*, 2006; *Gaudinski et al.*, 2000; *Phillips et al.*, 2013; *Randerson et al.*, 2002; *Schuur and Trumbore*, 2006].

Although terrestrial ecosystems contain carbon pools varying widely in turnover time and carbon age, most respiration is from carbon sources that have rapid turnover, including roughly 50% [*DeLucia et al.*, 2007] coming from autotrophic respiration that has a residence time on the order of days [*Bowling et al.*, 2002; *Högberg et al.*, 2001]. These rapidly cycled pools represent a small fraction of total terrestrial carbon, most of which is in soil pools with long turnover times [*Schlesinger and Andrews*, 2000; *Trumbore*, 2000]. The $\Delta^{14}C\text{-}R_{eco}$ is dominated by the turnover time of fast, rapidly cycled carbon pools and represents the "transit time" (in the sense of *Thompson and Randerson* [1999]) for the rapidly cycled carbon pool to return to the atmosphere. Nevertheless, monitoring changes in $\Delta^{14}C\text{-}R_{eco}$, as well as component fluxes from soil, can be an important indicator of changing flux sources and of the strength of carbon-climate feedbacks.

Modeling exercises to constrain the terrestrial $\Delta^{14}C$ disequilibrium have focused primarily on estimating heterotrophic, rather than autotrophic, respiration, because autotrophic respiration is dominated by recent photosynthates and should have comparatively little impact on atmospheric $\Delta^{14}CO_2$ [*Högberg et al.*, 2001; *Hopkins et al.*, 2013]. We argue, however, that there are at least two problems focusing on heterotrophic respiration to constrain terrestrial ecosystem C turnover. The first is that the $\Delta^{14}CO_2$ of heterotrophic respiration can only be isolated through disturbance, as in laboratory soil incubations [*Czimczik et al.*, 2006; *Gaudinski et al.*, 2000] or in trenched field plots to exclude roots [*Phillips et al.*, 2013], or isolated at times of year when plants are less active [*Phillips et al.*, 2013], and these constraints almost certainly introduce observational biases. For instance, *Ewing et al.* [2006] showed that soil disturbance tends to increase the apparent age of respired carbon. The second problem is that heterotrophic respiration cannot be assumed to be the only source of older, stored carbon. There is growing appreciation that stored plant carbon reserves are available for plant activity [*Carbone et al.*, 2013; *Richardson et al.*, 2013] and that in some ecosystems geologic CO_2 sources can also have appreciable influences on soil respiration [*Rey et al.*, 2012].

Sampling whole soil or ecosystem respiration, of which heterotrophic respiration is a component, is both a more practical and more complete measurement of biospheric ^{14}C emissions. Several studies have measured $\Delta^{14}C$-R_{eco} of low-stature systems using chambers [*Hardie et al.*, 2009; *Hicks Pries et al.*, 2013; *Lupascu et al.*, 2014], and at least one study has examined $\Delta^{14}C$-R_{eco} of a forest ecosystem from atmospheric measurements, albeit under disturbed conditions. *Schuur et al.* [2003] sampled $^{14}CO_2$ in air from a ridge above a boreal forest experimental burn to estimate the organic carbon pools that were consumed by fire. To our knowledge, no other measurements of $\Delta^{14}C$-R_{eco} have been made with atmospheric approaches in tall-canopy ecosystems. While *stable* isotope measurements of forest ecosystem respiration (i.e., $\delta^{13}C$-R_{eco}) are comparatively routine, barriers to $\Delta^{14}C$-R_{eco} measurements include high cost and the need for high analytical precision when attempting to resolve relatively small gradients in the atmosphere. The analytical limitations have been largely overcome by high-precision accelerator mass spectroscopy (AMS) preparation and measurement protocols, with $<2‰$ counting precision now routinely achieved at the Center for AMS at Lawrence Livermore National Laboratory (CAMS) in sample sizes equating to 2–4 L of whole air [*Graven et al.*, 2007], in contrast to the typical AMS precision of $\sim5‰$ [*Graven et al.*, 2007]. This makes atmospheric approaches to analyze near-surface isotopic gradients feasible.

We expected that two isotopic mixing model approaches could be practically applied for estimating forest $\Delta^{14}C$-R_{eco}. The first was to measure vertical gradients of CO_2 and ^{14}C between the ground and the forest canopy at night as respired CO_2 accumulated. The isotopic signature of added CO_2 can be estimated through the use of so-called "Keeling plot" analysis, which considers the relationship between measured concentrations and isotopic compositions (in the form $1/CO_2$ versus $\Delta^{14}C$). Ideally, to detect a well-mixed flux from soil and plants, one would want to make observations above the forest canopy under turbulent conditions. As shown by *Bowling et al.* [2005], however, the nocturnal range of CO_2 is small near the top of the canopy, which inflates the error in Keeling plot analysis. Constructing Keeling plots from vertical profiles from the ground to the top of the canopy gives a bigger range in CO_2 concentration and reduces statistical uncertainty, with the trade-off being that the influence of soil respiration may be overestimated relative to stem and foliar contributions due to the closer proximity of samples to ground level. Soil fluxes at Willow Creek are known to be a large portion of R_{eco}, however, and were previously estimated at 75% using scaled-up chamber measurements of soil, foliar, and stem respiration [*Bolstad et al.*, 2004]. We anticipated that the large soil flux contributions at WCR would enhance our ability to detect $\Delta^{14}CO_2$ of biospheric emissions in atmospheric measurements. Here we aimed to test the hypothesis that large soil contributions, particularly during the summer, would lead to a steep vertical gradient in $\Delta^{14}CO_2$ that would be large enough to analytically resolve $\Delta^{14}C$-R_{eco}. Such estimates may be biased toward $\Delta^{14}C$ of soil respiration [*Bowling et al.*, 2005], but biases can be quantified, as we attempt to do here.

Previous work in a northern deciduous forest in Massachusetts, USA, showed soil-respired $\Delta^{14}CO_2$ to be about 30‰ higher than ambient atmospheric $\Delta^{14}CO_2$ [*Gaudinski et al.*, 2000]. Based on the similar stand age at WCR, we expected enrichment from excess "bomb" ^{14}C in soil respiration and very little respiratory contribution from prebomb soil carbon. If we make the simplifying assumption that nocturnal CO_2 buildup is entirely derived from soil respiration, this would give a theoretical increase in canopy $\Delta^{14}CO_2$ of 0.08‰ per ppm (i.e., 30‰/380 ppm background CO_2 concentration). During active summer months, nocturnal CO_2 at WCR can be as much as 200 ppm higher at ground level than at the top of the canopy, giving an expected $\Delta^{14}CO_2$ range of as much as 16‰ above that of the ambient atmosphere, which would be readily detectable with high-precision methods. While forest CO_2 buildup is derived from both soil and aboveground plant respiration, stable nighttime conditions and high respiration rates can be expected to produce a large buildup of CO_2, with a large portion of respiration derived from soil fluxes so that $\Delta^{14}C$-$R_{eco} \approx \Delta^{14}C$-$R_s$.

In the second approach we employed observations at much larger spatial and temporal scales and applied an isotopic mixing model described by *Miller and Tans* [2003]. The Miller and Tans and Keeling plot approaches are both two-member mixing models, but the Miller and Tans approach is formalized for situations where background CO_2 concentration and isotopic composition vary through time. Using measurements from the nearby LEF tall tower as background, we subtracted LEF measurements from canopy observations at WCR to isolate local enhancements and analyzed regressions of residual $\Delta^{14}C$ and CO_2 to infer $\Delta^{14}C$-R_{eco}. While the subcanopy Keeling plot approach included observations from only two different overnight measurement campaigns, the canopy-minus-background approach made use of 86 paired observations over 20 months.

The primary objectives of this study are summarized as follows:

1. To test subcanopy and canopy-minus-background atmospheric approaches for estimating $\Delta^{14}C\text{-}R_{eco}$.
2. To compare $\Delta^{14}C\text{-}R_{eco}$ with previously reported total and heterotrophic soil-respired $\Delta^{14}CO_2$ at WCR (abbreviated $\Delta^{14}C\text{-}R_s$ and $\Delta^{14}C\text{-}R_h$, respectively).
3. To compare observations of $\Delta^{14}CO_2$ from WCR with estimates from the CASA model.

2. Methods

2.1. Willow Creek Site Description and Sampling

The Willow Creek AmeriFlux site (US-WCR, hereafter referred to as WCR) is located in the Chequamegon National Forest of north central Wisconsin (45°48′N, 90°07′W, elevation 515 m). The site is a mature, second-growth forest approximately 70–90 years old, dominated by deciduous hardwoods interspersed with conifer stands. Eddy covariance and profile CO_2 measurements have been made at the site since 1998 (further instrumentation details and site characteristics are described in *Bolstad et al.* [2004], *Cook et al.* [2004], and *Desai et al.* [2005]). The top of the forest canopy is approximately 25 m. During the growing season, it is estimated that 90% of the respiration flux measured by the eddy covariance system emanates from within 0.6 km of the flux tower [*Cook et al.*, 2004].

A year-round flask sampling program for $^{14}CO_2$ from an inlet height of 21 m above ground level took place from May 2011 to December 2012. Sampling frequency was every 5 days at 12:30 A.M. local time, plus additional sampling during the first growing season to characterize day-to-day and diurnal variability. In June and August 2012 we also identified two suitable nights for Keeling plot analysis when respiratory fluxes were large and near-term weather forecasts predicted no precipitation and low wind speed to ensure stable conditions through the sampling period, approximately 9 pm to 1 am local time. We sampled inlets from ground level to above the canopy, at 0.6, 1.5, 3, 7.6, 21, and 30 m heights.

For most samples, we collected air into two flasks in succession (<5 min apart) and compressed the samples using a programmable flask package to obtain approximately four standard liters [*Andrews et al.*, 2013]. This provided approximately 0.8 mg C for subsequent AMS analysis. For the June Keeling plot only, we used a single flask per sample (due to equipment limitations), which produced about 0.4 mg C for analysis. The samples were extracted and graphitized using high-precision methods [*Graven et al.*, 2007], but the smaller sample size provided only about 50–70% of the AMS ^{14}C counts normally measured for high-precision samples. The reduced number of ^{14}C counts, however, led to only a minor increase in analytical uncertainty. The AMS uncertainty was 2.3‰ for this group of small samples in comparison to 1.8‰ for full-sized high-precision process standards (Table S1 in the supporting information).

CO_2 concentrations were measured in the field directly using an LI-6262 closed path infrared gas analyzer (Licor Environmental, Lincoln, NE, USA) and an automated calibration system described by *Cook et al.* [2004]. Each profile height was sampled at 1 s frequency for 3 min every 21 min. The final minute of sampling was averaged, and these measurements were then interpolated to every 3 min using a cubic spline regression as described by *Cook et al.* [2004]. The LI-6262 compares the infrared absorption of the sample cell against a known reference standard, acquired from the NOAA Earth System Research Laboratory greenhouse gas program ($CO_2 = 445.84 \pm 0.1$ ppm). The reference was sampled against itself for 5 min every 42 min, and any zero offset was interpolated and subtracted from the air samples. Calibration curves were determined by interpolation of a second-order polynomial fit to 3-hourly sampling of three known reference standards (349.86, 445.84, and 548.14 ppm), application of ideal gas law pressure/temperature corrections, and previously characterized instrument drifts in calibration with temperature. After correction, we estimate an accuracy of 0.2 ppm. For the two Keeling plot sampling nights, concentrations were measured at each sampling height with the LI-6262 until a stable reading was achieved, immediately prior to filling the flasks.

In addition to these profile measurements, continuous measurements of soil respiration and periodic growing season measurements of soil-respired $\delta^{13}CO_2$ and $\Delta^{14}CO_2$ were collected from 2011 to 2012. These results and the associated methods were reported in detail by *Phillips et al.* [2013], and relevant comparisons to atmospheric measurements and the CASA model are presented here. Soil respiration was measured using forced diffusion chambers (FD, Forerunner Research, Dartmouth, NS, Canada) coupled with Vaisala

GMP343 CO_2 sensors (Vaisala Corp, Helsinki, Finland), a technique described in *Risk et al.* [2011]. For comparison to the CASA model estimates of heterotrophic respiration (R_h) for the 1° × 1° grid cell containing the WCR site, we present observations from a single trenched plot located about 30 m from the base of the eddy covariance tower. The trenched plot was established in September 2011 by digging a trench 30 cm wide × 100 cm deep around all sides of a 2 m × 2 m plot and lining it with 0.13 mm thick polyethylene vapor barrier to prevent ingrowth of new roots, before refilling with soil. The plot contained no trees or shrubs, and herbaceous plants were clipped to root crowns to prevent photosynthetic C inputs. An FD chamber at the center of the plot provided hourly measures of R_h for September 2011 to December 2012, and monthly averages are reported here. Periodic side-by-side comparisons between the FD system and a Licor-8100 soil flux system showed that the FD was biased to lower measurements than the Licor (FD μmol m^{-2} s^{-1} = 0.74 × Licor μmol m^{-2} s^{-1} − 0.34, R^2 = 0.65, N = 19); however, under field conditions it is difficult to ascertain which system is more accurate. Under laboratory conditions, the instrumental error of the FD system has been shown to be lower than the Licor system [*Lavoie et al.*, 2015], but at low flux rates we expect that the FD system may have been less accurate than the Licor, based on observations of more high flux "spikes" in the FD time series and on the fact that the FD flux is based on a differential measurement between two CO_2 sensors, each of which is susceptible to instrumental noise and drift. (Newer versions of the FD chamber remedy this problem by using a single CO_2 sensor.)

The isotopic composition of soil flux was measured during fall 2011 and subsequently every 3 weeks during the 2012 growing season, from both the trenched plot and three intact soil profiles. Soil surface isotopic flux was computed from subsurface $\Delta^{14}CO_2$ and $\delta^{13}CO_2$ profiles measured at interfaces of genetic horizons at depths of approximately 8, 15, 22, 30, 50, and 70 cm, using the soil respiration gradient method adapted for isotopologues, as derived by *Nickerson et al.* [2014].

2.2. LEF Site Description and Sampling

The LEF tall tower (45°56′N, N90°16′W, elevation 470 m) is a radio tower that uses the call letters WLEF, located outside of Park Falls, Wisconsin, approximately 21.5 km from WCR. It is one of eight towers in the NOAA-GMD tall tower measurement program, a complete description of which can be found in *Andrews et al.* [2013]. The inlet for flask samples used in this study was 396 m above ground level. Footprints describing the influence of surface emissions on samples obtained at this height are regional in scale, on the order of 10^5–10^6 km^2, with an estimated *e*-folding length for sensitivity to emissions of ~10^2 km [*Gloor et al.*, 2001; *Vasys et al.*, 2011]. LEF is surrounded by mixed temperate forest, including aspen, northern hardwood, and coniferous stands, as well as forested and shrub wetlands, and a relatively sparse population density [*Davis et al.*, 2003].

Both CO_2 and $\Delta^{14}CO_2$ were measured from flask samples as part of the NOAA analysis suite, which includes greenhouse gases, stable isotopic composition of CO_2, hydrocarbons, and halocarbons [*Andrews et al.*, 2013]. $^{14}CO_2$ was included in the flask analysis from 2010 to the end of 2012. For the first ~15 months of the study period samples were collected for $^{14}CO_2$ every ~3 days and thereafter once every ~6 days. Paired flasks were filled for each sampling event using programmable flask packages (PFPs), which provided sufficient air for >0.4 mg for $^{14}CO_2$ analysis after other mixing and isotope ratios were measured. Sampling at LEF occurred near midday between 12:00 and 14:00 local standard time, in contrast to 0:30 A.M. at WCR, because of the emphasis at LEF on studying regional emissions. The boundary layer is highest at midday, resulting in strong vertical mixing and a regionally representative signal, which is also more likely to be well simulated by an atmospheric model.

2.3. Sample Preparation and AMS

Flasks from WCR were sent to the CAMS for cryogenic extraction of CO_2 from whole air, and LEF flasks were sent to the University of Colorado Institute of Arctic and Alpine Research (INSTAAR) Laboratory for AMS Radiocarbon Preparation and Research (NSRL), where an automated cryogenic extraction line was used [*Turnbull et al.*, 2009]. Purified CO_2 from both WCR and LEF was graphitized and analyzed at CAMS using high-precision methods described by *Graven et al.* [2007]. CO_2 was reduced to graphite on iron powder in the presence of H_2, and ^{14}C abundance was measured by atom counting on a HVEC FN Tandem Van de Graaff accelerator mass spectrometer.

Measurement uncertainty is described from long-term repeated measurements of whole air process standards, with two to three standards extracted, purified, and graphitized alongside each batch of authentic samples.

Whole air process control samples with CO_2 concentrations and $\Delta^{14}C$ near ambient levels were collected from high-pressure cylinders in individual extraction aliquots as described by *Lehman et al.* [2013] or, in the case of extractions performed at CAMS, from PFPs filled from cylinders. The control gases extracted at CAMS, which are identified as LARS1 and LARS2, had a standard deviation of 3.4‰ $\Delta^{14}C$ ($N = 23$, Table S1 in the supporting information). The standards extracted at the INSTAAR Laboratory, identified as NWT3 and NWT4, had a standard deviation of 2.4‰ ($N = 192$) (B. W. LaFranchi et al., Strong regional signature of boreal soil CO_2 emissions observed from a tall tower over the midwestern United States, *Geophysical Research Letters*, in review, 2015). The extra uncertainty for the CAMS-extracted samples is related to the extraction procedure and is currently under investigation. An ongoing intercomparison of atmospheric $^{14}CO_2$ measurements among AMS facilities showed that there is no detectable bias between CAMS results and those from other labs [*Miller et al.*, 2013].

Radiocarbon measurements are expressed in Δ notation in units of per mil (‰), measured relative to NBS Oxalic Acid I (OX1), with corrections for mass-dependent fractionation based on off-line $^{13}C{:}^{12}C$ measurement (normalized to a $\delta^{13}C$ of -25‰) and for radioactive decay between the time of sampling and measurement (see *Stuiver and Polach* [1977] and updated nomenclature in *Trumbore* [2009]). The $\delta^{13}C$ values for WCR were analyzed on CO_2 splits by the UC Davis Stable Isotope Laboratory (GVI Optima Stable Isotope Ratio Mass Spectrometer). The $\delta^{13}C$ values for LEF were measured at the INSTAAR Stable Isotope Laboratory [*Vaughn et al.*, 2004]. Uncertainty for $\delta^{13}C$ is estimated at less than 0.1‰ for both laboratories.

2.4. Data Analysis

We used two techniques for estimating $\Delta^{14}C$-R_{eco} at WCR: (1) a subcanopy approach, regressing vertical profile $\Delta^{14}C$ versus $1/CO_2$ in a Keeling plot [*Keeling*, 1958], and (2) a canopy-minus-background approach using the Miller-Tans mixing model [*Miller and Tans*, 2003], with observations from LEF as background and from WCR at the 21 m height as an assumed mixture of background atmosphere and local emissions from ecosystem respiration. The temporal and spatial scales of these techniques are quite different, with individual Keeling plot constructed from each of two single nights of observations and the Miller-Tans plots constructed from 20 months of observations.

Both mixing models are based on the theory that observed CO_2 is a combination of background atmosphere with a well-mixed source of CO_2 added to it. For Keeling plots, the observed $\Delta^{14}C$ in the canopy is expressed as follows:

$$\Delta_{obs} = C_{bkg}\left(\Delta_{bkg} - \Delta_{eco}\right)\left(\frac{1}{C_{obs}}\right) + \Delta_{eco} \tag{1}$$

where the subscripts obs, eco, and bkg represent the profile observations, R_{eco} source, and the background atmosphere, respectively, and Δ and C represent the ^{14}C abundance and CO_2 concentration, respectively. We solved for the intercept, Δ_{eco} by regressing profile $\Delta^{14}C$ (Δ_{obs}) versus $1/C_{obs}$, using ordinary least squares as recommended by *Zobitz et al.* [2006]. Our approach of using vertical profiles for Keeling plot analysis was similar to that of *Bowling et al.* [2005]. Due to the limited number of samples and the limited CO_2 gradient in the upper canopy, however, we combined all observations in a single regression rather than analyzing near-ground and upper canopy observations separately.

Because soil and foliage respiration sources are likely to be vertically stratified rather than well mixed [*Van Gorsel et al.*, 2009; *Thomas et al.*, 2013], combining observations from all heights into a single Keeling plot complicates interpretation of $\Delta^{14}C$-R_{eco} estimates. To assess the impacts to Keeling intercept calculations of sampling from a stratified CO_2 profile in contrast to a well-mixed source, we performed a sensitivity analysis with simulated data. Using the CO_2 concentration profiles observed on the two different nights (30 June to 1 July and 25–26 August, Figure 1), we produced expected $\Delta^{14}CO_2$ profiles for three different hypothetical scenarios (Figure 2), assuming that CO_2 in excess of background atmospheric concentrations was derived from either (1) only R_s, (2) a stratified mixture of R_s and foliar respiration (R_f), with the contribution from R_s decreasing linearly with canopy height from 100% at the soil surface to 0% at 21 m, or (3) an even mixture of R_s and R_f, with R_s contributing 75% of excess CO_2 at all canopy heights. For these simulations we assumed a background atmosphere of $CO_2 = 380$ ppm and $\Delta^{14}CO_2 = 30$‰ based on LEF mean values for 2011; $\Delta^{14}C$-$R_f = 30$‰, (i.e., the same as the background atmosphere); and $\Delta^{14}C$-$R_s = 54.6$‰ in June and 45.6‰ in August, as measured previously from soil chambers (see Figure 5).
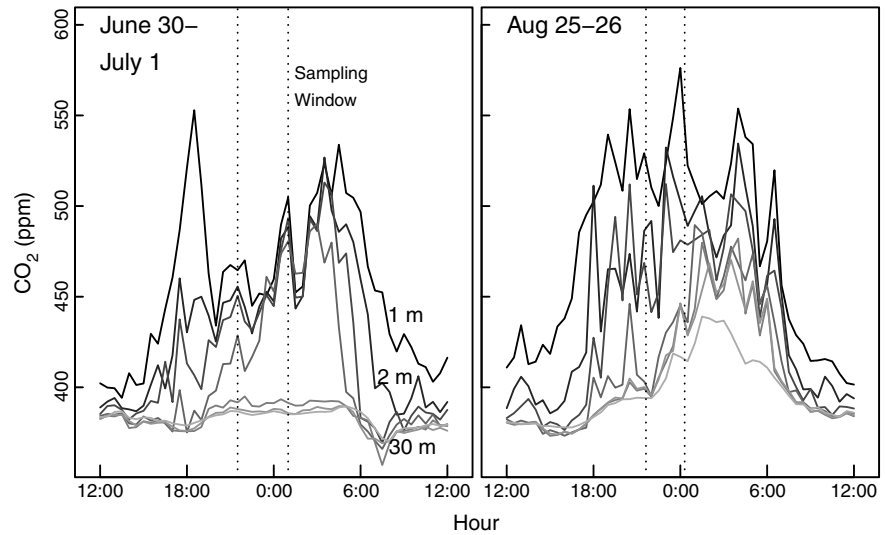
Figure 1. WCR profile CO_2 concentrations for 24 h period around Keeling plot sampling campaigns. The darkest line is closest to ground surface (1 m), and the lightest line is the highest sampling inlet, at 30 m.

For the canopy-minus-background approach, the relationship of observed CO_2 to background and source air is expressed as follows:

$$\Delta_{obs}C_{obs} - \Delta_{bkg}C_{bkg} = \Delta_{eco}\left(C_{obs} - C_{bkg}\right) \tag{2}$$

In this expression, which is a rearrangement of equation (1), $\Delta^{14}C\text{-}R_{eco}$ is given by the slope Δ_{eco}, time-varying background ("bkg") values of CO_2 and ^{14}C are from LEF, and the "obs" are the canopy observations. Because sampling days were asynchronous at WCR and LEF, we used loess fitting procedures (localized polynomial regressions) to interpolate LEF measurements to the date and time of WCR measurements. We fit equation (2) using ordinary least squares regression as recommended by *Zobitz et al.* [2006] to solve for the slope.

We also compare our observed $\Delta^{14}C$ values to estimates of $\Delta^{14}C\text{-}R_h$ derived from the CASA model. In the CASA model, the age distribution of heterotrophic respiration is estimated using impulse-response functions
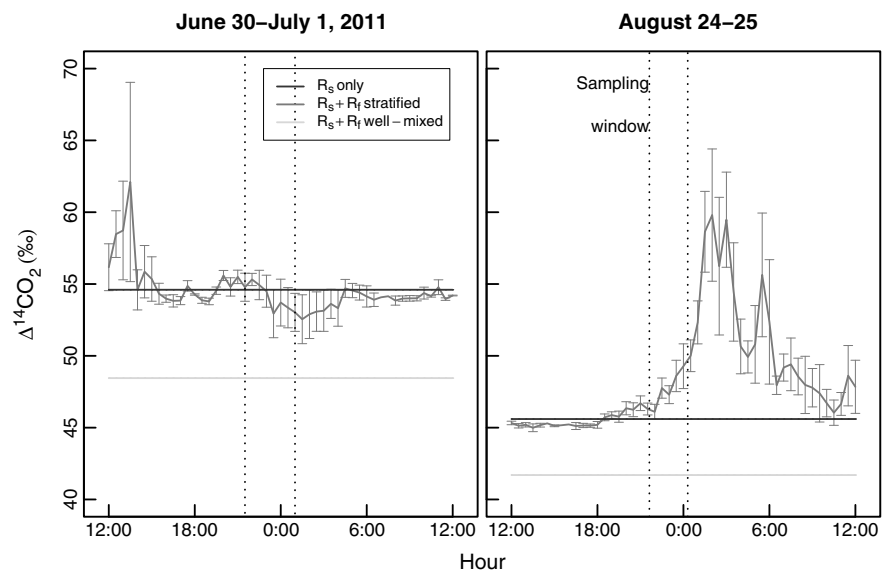

Figure 2. Expected Keeling intercepts for three hypothetical sources of biospheric $\Delta^{14}CO_2$, using observed CO_2 profiles from June and August sampling events. We assumed a background atmosphere of $CO_2 = 380$ ppm and $\Delta^{14}CO_2 = 30$‰, $\Delta^{14}C\text{-}R_f = 30$‰, and $\Delta^{14}C\text{-}R_s = 54.6$‰ in June and 45.6‰ in August, as measured from soil chambers.
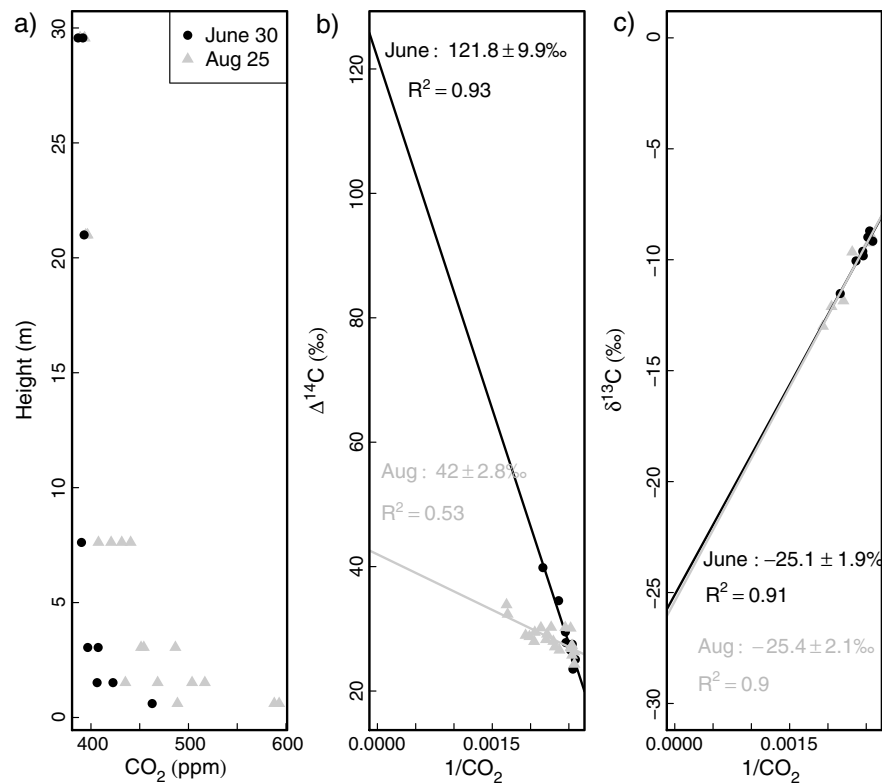
Figure 3. (a) Observed CO_2 profiles, (b) $\Delta^{14}C$ Keeling plots, and (c) $\delta^{13}C$ and $\Delta^{14}C$ Keeling plots for nights of 30 June to 1 July, and 25–26 August 2012. $N = 9$ for June ^{14}C and ^{13}C, $N = 12$ for August ^{14}C, and $N = 6$ for August ^{13}C (splits were taken from only one sample per height). Keeling intercept ± SE is shown.

[*Thompson and Randerson*, 1999]. Monthly varying ^{14}C isotopic disequilibrium for the $1° \times 1°$ grid cell surrounding LEF was calculated by convolving the modeled age distribution of heterotrophic respiration with the Northern Hemisphere atmospheric history of $\Delta^{14}C$ [*Hua*, 2013], as presented in *Miller et al*. [2012].

3. Results

3.1. Subcanopy Approach

Stable nocturnal conditions produced an accumulation of CO_2 below the WCR canopy on the nights of both sampling events, providing suitable sampling conditions for Keeling plot analysis (Figure 1). Concentration profiles in June, however, suggested that CO_2 in the upper canopy was decoupled from the subcanopy, a condition that frequently occurs in tall forest canopies during calm, stratified, low-turbulence conditions [*Van Gorsel et al*., 2009]. CO_2 concentrations remained low and stable at the top of the canopy throughout the night and accumulated only in the subcanopy. In August, CO_2 accumulation occurred at all heights. The vertical CO_2 range in August exceeded 200 ppm, in contrast to just 90 ppm in June.

Sensitivity analyses were conducted to assess how stratification of respiration sources and differences in sampling conditions on the two nights might influence Keeling intercepts (Figure 2 and Figure S1 in the supporting information). When we assumed a well-mixed source of CO_2, from R_s alone or from an evenly mixed 25/75% combination of R_f and R_s, Keeling intercepts recovered the source $\Delta^{14}CO_2$ signature accurately with no bias, regardless of differences in CO_2 stratification on the two sampling nights. (Note that we did not simulate random error in CO_2 or $\Delta^{14}C$ measurements, both of which would have increased the error of the Keeling intercepts in June, due to smaller CO_2 gradients.) In contrast, when we assumed that CO_2 from R_s and R_f were stratified in the canopy, Keeling intercepts were biased from an even mixture and were very similar to $\Delta^{14}C$-R_s. In June, the Keeling intercepts were indistinguishable from $\Delta^{14}C$-R_s within statistical errors, ranging from -0.4 to $+2$‰ of the prescribed $\Delta^{14}C$-R_s, and in August they were higher than $\Delta^{14}C$-R_s by
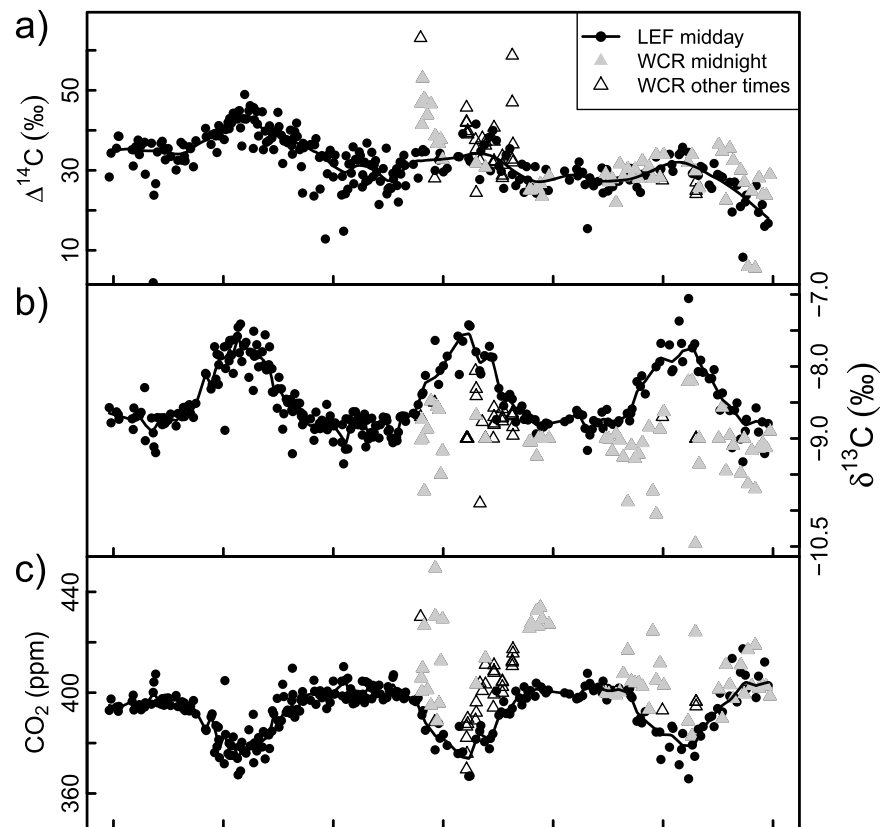
Figure 4. Series of (a) $\Delta^{14}CO_2$, (b) $\delta^{13}CO_2$, and (c) bulk CO_2 at LEF and WCR sites. LEF samples (black circles) were collected midday between 12:00 and 14:00 local time. WCR samples were collected at 0:30 local time (solid grey triangles), supplemented by samples at other times of day (empty triangles). Solid lines show loess fit for LEF observations, used to interpolate to WCR sampling days. Error bars are not shown for clarity: $\Delta^{14}C$ AMS error ≤ 2.5‰, $\delta^{13}C$ instrumental error <0.1‰, and CO_2 instrumental error was 0.1 ppm for LEF and 0.2 ppm for WCR.

0.4–3.7‰. Under the stratified scenario, there were also inflated errors in Keeling intercepts due to nonlinearity in Keeling plots (Figure S1 in the supporting information). Nonlinearities occurred because CO_2 buildup in the upper canopy was dominated by respiration with a $\Delta^{14}C$ signature the same as the background atmosphere, whereas CO_2 buildup near the soil surface had a $\Delta^{14}C$ signature distinct from the atmosphere.

We also examined how stratification of respiration sources can affect $\delta^{13}C$-R_{eco} estimates. We assumed enrichment in foliar respiration of 5‰ more than soil respiration, based conservatively on upper end differences reported by previous studies [*Bowling et al.*, 2005; *Ogée et al.*, 2003]. As for $\Delta^{14}C$, Keeling intercepts were similar to $\delta^{13}C$-R_s for the stratified scenario, differing from $\delta^{13}C$-R_s by +0.007 to −0.25‰ in June, and −0.2 to −1.4‰ in August (data not shown).

The Keeling intercepts based on actual profiles were 121.8‰ (SE = 9.9, R^2 = 0.93) in June and 42‰ (SE = 2.8, R^2 = 0.53) in August (Figure 3). For comparison, the mean atmospheric $\Delta^{14}CO_2$ at LEF from June to August 2012 was 31.8‰, which by subtraction gives $\Delta^{14}C$ disequilibria with respect to atmosphere of 90‰ and 10‰ for the June and August nights, respectively. This results in a mean age of R_{eco} for June of 16–19 years, and for August of 1–4 years, based on measurements of tropospheric $^{14}CO_2$ for the appropriate Northern Hemisphere zone [*Hua*, 2013] and from Niwot Ridge [*Lehman et al.*, 2013]. (See methods for age determination in the supporting information.) Keeling intercepts for $\delta^{13}C$ were −25.1‰ in June (SE = 1.9‰, R^2 = 0.91) and −25.4‰ in August (SE = 2.1‰, R^2 = 0.90).

3.2. Canopy-Minus-Background Approach

Figure 4 shows observations of $\Delta^{14}C$, $\delta^{13}C$, and CO_2 for LEF and WCR from 2010 to 2012. LEF observations exhibit seasonal cycles consistent with those found at other atmospheric monitoring sites [e.g., *Graven et al.*, 2012;
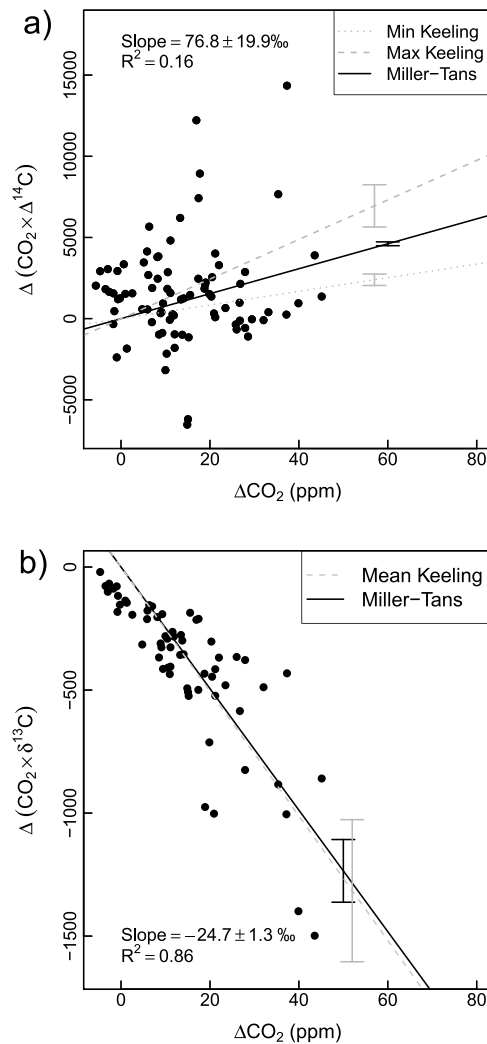
Figure 5. Miller-Tans plots for (a) $\Delta^{14}C$ and (b) $\delta^{13}C$. $\Delta^{14}C$-R_{eco} and $\delta^{13}C$-R_{eco} are given by the slopes of the black fitted lines (equation (2)), and slope $\pm$ SE and R^2 values are given for those regressions. For method comparison, grey lines show mixing relationships that would be expected based on the subcanopy Keeling estimates of R_{eco}. In Figure 5a, minimum Keeling estimate of $\Delta^{14}C$-R_{eco} was 57.0‰ from August sampling event, and maximum Keeling estimate was 121.8‰ from June sampling event. A single error bar for each mixing line is shown at the upper end of the observed ΔCO_2 range, indicating the 95% confidence interval for the slope.

Levinet al., 2010]. In particular, CO_2 was lower and $\delta^{13}C$ was higher in summer than winter due to photosynthetic uptake, and $\Delta^{14}C$ was higher in summer than winter, which is thought to be related to terrestrial respiration as well as influx of ^{14}C from the stratosphere, which peaks seasonally in late spring [*Randerson et al.*, 2002]. Proximity to the forest canopy produced more depleted $\delta^{13}C$ and higher CO_2 concentrations at WCR than LEF, reflecting CO_2 contributions from plant and soil respiration. Contrary to expectation, however, $\Delta^{14}C$ values at WCR only show enrichment attributable to terrestrial respiration of excess ^{14}C for a brief period in early summer 2011. Subsequent observations from the late summer through winter and the following growing season showed similar $\Delta^{14}C$ at the two locations.

Subtracting LEF from WCR observations produced residual $\Delta^{14}C$, $\delta^{13}C$, and CO_2 values that were used to fit the Miller-Tans mixing model (equation (2)), with mixing relationships shown in Figure 5. The scatter in $\Delta(\Delta^{14}C \times CO_2)$ and $\Delta(\delta^{13}C \times CO_2)$ versus ΔCO_2 relationships was large, but nevertheless, the slopes were significant when zero-intercept models were assumed. Estimated $\Delta^{14}C$-R_{eco} based on the slope of Miller-Tans regressions was 76.8‰ (SE = 19.0‰, $p < 0.001$, $R^2 = 0.16$). This value is intermediate between the June and August Keeling intercepts and is equivalent to a flux-weighted C age of approximately 4–12 years. Estimated ^{13}C-R_{eco} was −24.7‰ (SE = 1.3, $p < 0.001$, $R^2 = 0.86$), which is indistinguishable within error limits from the results obtained using the subcanopy approach.

We also examined the sensitivity of residuals and associated regressions to different specifications of the loess fitting window, varying it within a range that appeared reasonable by visual inspection and to using linear interpolation rather than loess fitting. We found only minor impacts on estimated $\Delta^{14}C$-R_{eco} (<4‰ $\Delta^{14}C$)

and $\delta^{13}C$-R_{eco} (<0.5‰ $\delta^{13}C$) from adjusting the fit. The sensitivity of estimated ecosystem C age to these adjustments was < 1 year.

3.3. Comparison of $\Delta^{14}C$-R_{eco} to Soil Observations and Model Estimates

Figure 6 compares $\Delta^{14}C$-R_{eco} at WCR to $\Delta^{14}C$ of total soil respiration, heterotrophic soil respiration from a trenched plot, and to $\Delta^{14}C$ of heterotrophic respiration derived from the CASA Earth system model for the 1°×1° grid cell region containing WCR and LEF. As previously reported, soil-respired $\Delta^{14}C$ from intact plots had a decreasing trend over the growing season as new photosynthates were respired, whereas $\Delta^{14}C$-R_h from the trenched plot was variable but had no seasonal trend [*Phillips et al.*, 2013]. Atmospheric measurements of $\Delta^{14}C$-R_{eco} were within the range of $\Delta^{14}C$ values found for soil fluxes, with the exception of

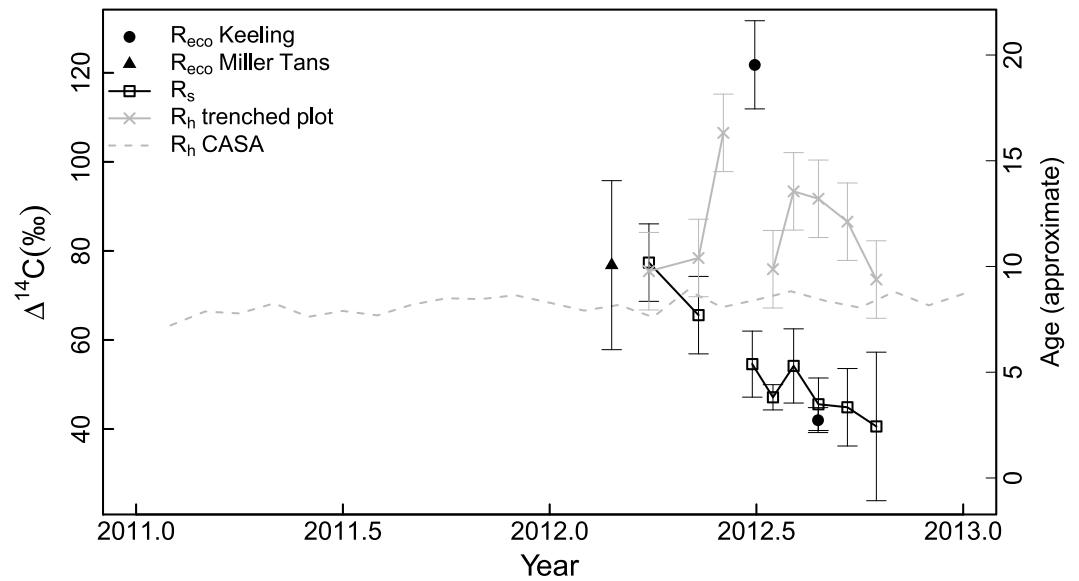**Figure 6.** Time series of WCR Δ^{14}C-R_{eco}, Δ^{14}C-R_s, Δ^{14}C-R_h, and CASA modeled Δ^{14}C-R_h for the 1° × 1° grid cell containing LEF and WCR. ^{14}C-R_s was measured from three soil plots, and Δ^{14}C-R_h was measured from one trenched soil plot [*Phillips et al.*, 2013]. The canopy-minus-background approach for estimating Δ^{14}C-R_{eco} integrated observations from the entire measurement period and is arbitrarily shown at the midpoint of observations in early 2012.

the June Keeling intercept, which exceeded Δ^{14}C from both intact and trenched soil plots. The August Keeling intercept was similar to soil-respired Δ^{14}CO$_2$ sampled from intact plots during the same time period. The Miller-Tans estimate of Δ^{14}C-R_{eco} was similar to average heterotrophic Δ^{14}C from the trenched plot over the measurement period (85.2‰, $1\sigma = 11.5$‰, $N = 8$).

CASA estimates of heterotrophic Δ^{14}C had no seasonal trend, which is consistent with observations from the trenched plot. While CASA captured the lack of seasonal trend, it substantially underestimated mean Δ^{14}C-R_h. CASA Δ^{14}C-R_h values averaged 68.6‰ (SD = 1.93‰) in 2012, which was 5 to 38‰ less than observed Δ^{14}C-R_h, and equivalent to 1–10 years younger than observed Δ^{14}C-R_h. In contrast, CASA estimates of heterotrophic bulk CO$_2$ flux rates were very similar to observations from the trenched plot (Figure 6).

3.4. Fossil Versus Biospheric CO$_2$ Influences at Canopy and Tall Tower Spatial Scales

A final analysis compared the long-term (2011–2012) mixing relationships between Δ^{14}C and CO$_2$ at the LEF and WCR towers, to see if the relative importance of emission sources at the two spatial scales differed (Figure 8). The general trend for both sites was a decrease in Δ^{14}C as CO$_2$ concentration increased, indicating that ^{14}C-free fossil fuel-derived CO$_2$ is an important source of CO$_2$ at both spatial scales. For comparison, Figure 8c shows theoretical mixing lines for the hypothetical case in which all CO$_2$ is derived from fossil fuel combustion (in which Δ^{14}C would be expected to decrease by −2.6‰ per ppm CO$_2$) or from biospheric respiration (in which Δ^{14}C would be expected to increase by 0.03 to 0.24‰ per ppm CO$_2$, based on minimum and maximum estimates of ^{14}C-R_{eco}). The steep negative slope for LEF during winter shows that fossil influences are particularly significant during the dormant period (October–April) in contrast to the growing season (May–September). There was a distinct decrease in slope at LEF from the dormant to the growing season, which indicated a change in CO$_2$ sources and potentially greater biospheric influence. Importantly, a seasonal shift was not apparent at the WCR tower, suggesting that local respiration was more important at the canopy scale year-round, though respiration emissions appear to have been overprinted by fossil influences.

4. Discussion

4.1. Comparison of ^{14}C-R_{eco} Measurement Approaches

We estimated Δ^{14}C-R_{eco} at 42.0‰ and 121.8‰ Δ^{14}C using the subcanopy approach and 76.8‰ Δ^{14}C using the canopy-minus-background approach. For the subcanopy approach, we learned through the sensitivity analysis

that the stratification of respiration sources biased Keeling intercepts toward $\Delta^{14}C\text{-}R_s$, leading to overestimates of $\Delta^{14}C\text{-}R_{eco}$. Stratification would have particularly affected the June Keeling intercept, because CO_2 concentration profiles indicated that there was decoupling between the subcanopy and the canopy (Figure 1). Instead of a gradual increase in CO_2 with height, concentrations moved into distinct subcanopy and upper canopy regimes near midnight, with soil CO_2 emissions pooling near-ground level.

The June Keeling intercept even exceeded observations of $\Delta^{14}C\text{-}R_s$, however (Figure 6). One possible explanation for this very high value is that the area immediately around the base of the tower is disturbed and has less vegetation and may have had higher levels of heterotrophic respiration. $\Delta^{14}C\text{-}R_h$ was found to be as high as 106.8‰ in spring 2012. Another possible explanation is that stratification caused nonlinearity in Keeling plots, inflating the error in the Keeling intercept estimate. Our sensitivity analysis indicated an error of only 0.4–2‰ from a pure soil source, but the actual error could have exceeded our simulations. Error inflation in Keeling intercepts resulting from profile stratification has been shown by others in modeling simulations for subcanopy $\delta^{13}C$ [*Baldocchi and Bowling*, 2005].

The August sampling night represented more ideal conditions for Keeling plot analysis, with CO_2 profiles showing higher CO_2 accumulation at all heights and a more gradual change in concentration with height, which suggested that CO_2 transport was primarily across the gradient and no significant counter-gradient flows. We can still expect under these conditions that R_s had a large influence on Keeling intercepts, but we can also expect that soil respiration would have moved out of the subcanopy and into the upper canopy, which would reduce the nonlinearity in Keeling plots. In addition, the larger CO_2 range across the profile should reduce Keeling intercept uncertainty, as shown by others for $\delta^{13}C$ [*Bowling et al.*, 2005; *Pataki et al.*, 2003]. The Keeling intercept in August was similar to soil estimates of $\Delta^{14}C\text{-}R_s$ from the same time (which averaged 45.6‰, SD = 5.9‰).

Taking together the comparisons of tower and soil measurements, and the sensitivity analysis that suggests Keeling intercepts are biased toward R_s, we recommend that the subcanopy $\Delta^{14}C\text{-}R_{eco}$ estimates are best interpreted as tower-based measures of $\Delta^{14}C\text{-}R_s$. Our original hypothesis, that large soil contributions during the summer would lead to a steep vertical gradient in $\Delta^{14}CO_2$ that would be large enough to analytically resolve a source $\Delta^{14}C$ signature from atmospheric measures, proved correct.

An alternative sampling approach which has been used for $\delta^{13}C\text{-}R_{eco}$ analysis to address stratification of respiration sources is to separate Keeling plots for different heights. We expect, however, that Keeling intercepts would be difficult to solve in the upper canopy, because respiration would be dominated by plant respiration that has similar ^{14}C abundance to the background atmosphere, resulting in a weak linear relationship between $1/C_{obs}$ and Δ_{obs}. We collected diurnal measurements in summer 2011 at the 21 m height to evaluate this approach (Figure 4, unfilled triangles). We collected samples every 2 h on five separate nights from August to October and found no relationship between CO_2 concentration and $\Delta^{14}C$ (relationships not shown). Because plant respiration sources are stratified from soil sources and similar to background $\Delta^{14}C$, Keeling approaches are poorly suited to capturing foliar contributions.

Although subcanopy measurements do not appear to capture a well-mixed sample of $\Delta^{14}C\text{-}R_{eco}$, there is nevertheless utility in using this approach to estimate $\Delta^{14}C\text{-}R_s$. Tower-based measurements integrate soil respiration over a much larger spatial scale than chamber or subsurface soil flux measurements, which sample an area generally $< 100\,cm^2$ and are spatially heterogeneous. The area represented by the Keeling plots is estimated to be on the order of about $500\,m^2$, based on the product of the average wind speed and the sample integration time. The value of monitoring R_s is underscored by the fact that it is estimated to be the largest component of R_{eco} and is the component that is most susceptible to change in response to disturbance or climate change because of large pools of stored soil C.

The stratification of respiration sources and decoupling of subcanopy and canopy fluxes can be expected to produce artifacts in Keeling $\delta^{13}C$ estimates as well, but the errors are comparatively small, estimated at approximately 0–1.4‰. Our sensitivity analysis presented a worst-case scenario, with larger differences between foliar and soil-respired $\delta^{13}C$ than are typically measured with chambers [*Tu and Dawson*, 2005]. The comparatively high R^2 values for $\delta^{13}C$ Keeling plots and good agreement between both sampling events is due to the relative uniformity in the $\delta^{13}C$ of forest respiration sources. The subcanopy and canopy-minus-background approaches also had good agreement for $\delta^{13}C$, despite the large differences in spatial and temporal scales
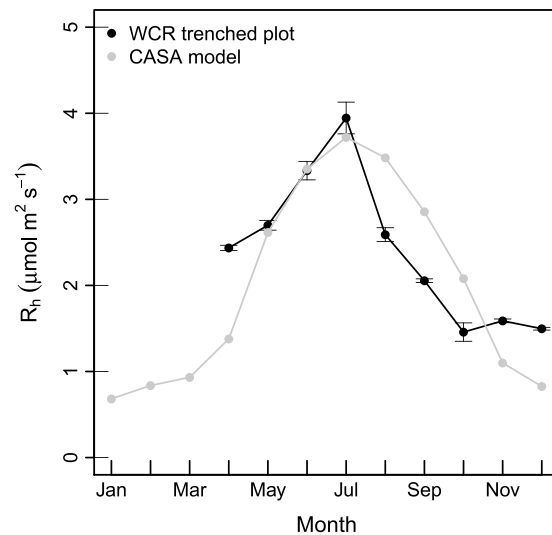
Figure 7. Comparison of mean monthly heterotrophic respiration rate calculated with CASA versus observations from WCR trenched plot.

(mean for the subcanopy approach was -25.3 ± 2.0‰ and -24.7 ± 1.9‰ for the canopy-minus-background approach). These values are also similar to the findings from a survey of nocturnal Keeling plots from flask measurements for 17 other temperate deciduous forests, which had an average ^{13}C-R_{eco} of approximately -25 ± 1‰ [*Pataki et al.*, 2003].

The canopy-minus-background approach also had limitations stemming from the assumption of a well-mixed CO_2 emissions source. At this large spatial scale, regional fossil emissions in addition to biospheric emissions can influence atmospheric $\Delta^{14}CO_2$. Fossil emissions were apparent at both the WCR and LEF towers but had more influence on the observations at LEF, as indicated by the more negative slope at LEF than WCR in Figure 8. When LEF background levels were subtracted from WCR in the Miller-Tans mixing model (Figure 5), the fossil influences were largely removed and the Miller-Tans model had a positive slope, showing dominant biogenic influences, but variance was high and R^2 was only 0.16. This variance was likely a combination of analytical uncertainty (i.e., AMS error) and random environmental error that could include mismatch between atmospheric sampling conditions at LEF and WCR.

Bowling et al. [2005] advised caution when using measurements from large spatial scales as background values for canopy-level mixing models, reporting that samples from 10 m above the forest canopy were considerably different from synchronous samples above a neighboring short canopy site and from aircraft observations. Over synoptic to seasonal timescales, however, we expect LEF to reflect trends in the CO_2 concentration and isotopic composition in the boundary layer above the WCR canopy [*Desai et al.*, 2010; *Helliker et al.*, 2004]. This is supported by the fact that $\Delta^{14}CO_2$ for LEF and WCR track together through time (Figure 4). Furthermore, by using loess fits of the LEF observations, we effectively subtracted multiday means from WCR, rather than individual LEF observations. The use of long-term data to construct the Miller-Tans mixing model also helps to average out random differences between LEF and background conditions in the boundary layer above WCR.

We did observe, however, a clear shift in CO_2 sources at LEF from dormant to growing season months that was not apparent at WCR, based on ^{14}C versus CO_2 mixing relationships (Figure 7). B. W. LaFranchi et al. (in review, 2015) investigated the cause of the seasonal shift at LEF and concluded that soil respiration, not only from WCR but from a broader region of boreal forest in Canada, is likely contributing to the summer increase in atmospheric $^{14}CO_2$. This finding suggests that the seasonal shift at LEF is related to an enhanced respiratory signal in summer and to fossil signals dominating in winter. The divergent seasonal patterns at WCR and LEF in Figure 8 are likely due to the stronger influence of local sources at WCR, which are dominated by respiration but may also include occasional fossil sources (e.g., from vehicles, recreation, and timber activities in the forest) and influences of regional CO_2 sources at LEF, which include year-round fossil emissions and seasonally important emissions from respiration sources. The seasonal shift in sources at LEF does not necessarily mean it is less suitable as a background site in winter, but it does indicate weaker impacts from respiration, which is to be expected since respiration rates are also lower in winter.

4.2. Turnover Time of Whole Ecosystem Forest Carbon

We estimated a range in age of respired CO_2 ranging from 1 to 19 years with the subcanopy approach and 4–12 years with the canopy-minus-background approach. The upper estimate of 19 years, derived from the June 2012 subcanopy sampling event, is less reliable due to stratified sampling conditions. The age range for soil respiration from intact soil plots was 0–7 years, and a more conservative estimate for
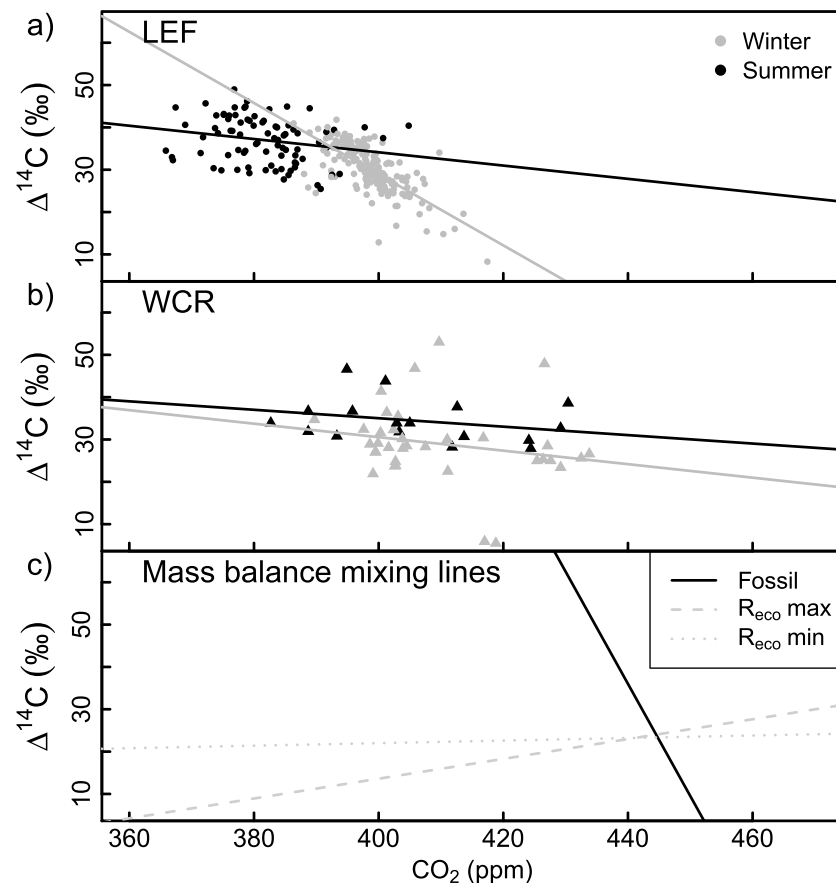
Figure 8. $\Delta^{14}CO_2$ versus CO_2 at (a) LEF and (b) WCR, and (c) hypothetical mixing lines assuming all CO_2 derives from fossil or respiration sources. In Figure 8c R_{eco} maximum was 121.8‰ from the June Keeling estimate, and R_{eco} minimum was 57.0‰ from the August Keeling estimate.

$\Delta^{14}C$-R_{eco} should fall within this range because foliar respiration is not expected to contribute older carbon than soil respiration.

We interpret the ^{14}C age for R_{eco} following the approach used for modeling of soil turnover [*Trumbore*, 2000], which is to assume that the age of respired carbon reflects the mean turnover time of the metabolically active carbon reservoir. We can conclude that the actively cycling carbon at WCR is less than 20 years old, while much of the forest carbon reservoir, particularly stored soil carbon, turns over at considerably slower rates.

Until recently, the disequilibrium in age between CO_2 taken up and released by ecosystems was thought to be related primarily to respiratory contributions from heterotrophs turning over soil carbon. Recent work, however, suggests that isotopic disequilibrium may also be influenced by plant mobilization of stored carbon, challenging the assumption that autotrophic respiration derives from current year photosynthates. Plant starches, a putative respiratory substrate, were found to have a mean age of 7–14 years at three northern hardwood forests [*Richardson et al.*, 2013]. Root respiration for a number of temperate deciduous forest sites has also been shown to derive from previous years' carbon, particularly early in the growing season [*Hopkins et al.*, 2013].

Radiocarbon-based estimates of not only soil carbon but also plant and whole ecosystem turnover serve as important observational constraints on Earth system models. For instance, variations in carbon residence time were recently shown to account for more than 30% of the variability in predicted 21st century changes in vegetative carbon storage for seven global vegetation models [*Friend et al.*, 2014]. We found that the CASA model estimates for the 1° × 1° grid cell region containing WCR had an excellent match to observed heterotrophic respiration rates, but estimated carbon age was 1–10 years younger than observed. It is worth noting that heterotrophic respiration is typically measured from lab incubations of disturbed soil and that $^{14}CO_2$ from the

trenched plot was considerably younger than $^{14}CO_2$ measured from lab incubations of the same soil [*Phillips et al.*, 2013]. Using the trenched plot to estimate ^{14}C-R_h thus brought the model and observations closer than using typical incubation techniques. Either a lack of plant storage processes or insufficient turnover of old soil carbon in the CASA model could have resulted in underestimated ages of $\Delta^{14}C$-R_h.

5. Conclusions and Recommendations

This study demonstrated that both subcanopy and canopy-minus-background approaches can be used to estimate biospheric $\Delta^{14}C$ in a tall-canopy forest ecosystem. More work is needed, however, to assess the extent to which subcanopy approaches can capture foliar respiration and to which fossil emissions complicate source estimates using the canopy-minus-background approach. These early findings are nevertheless promising, and we suggest that future studies replicate our efforts at other forest sites to refine methods and to ultimately increase the number of observations available for validating terrestrial carbon models.

Both approaches required high-precision AMS techniques ($<2‰$ uncertainty), large sample numbers, and careful selection of sampling conditions. In addition to these requirements, we suggest that future work improve on our methods in several ways. First, for the subcanopy approach, continuous measurements of profile $\delta^{13}C$ would be very useful for diagnosing stratification of respiration sources and identifying optimal sample timing, as well as verifying flask-based Keeling estimates of $\delta^{13}C$. Continuous, high-precision $\delta^{13}C$ measurements might also allow foliar and soil contributions to be estimated through non-Keeling approaches, for instance, using inverse Lagrangian analysis, as demonstrated by *Raupach* [2001]. Second, we suggest sampling on more nights to capture seasonal variability. One advantage of the subcanopy approach is that a source signature can be estimated over a single night, so changes can be monitored over the course of a growing season. Future efforts also require careful selection of sampling locations. Ideal locations for the subcanopy approach are tall plant canopies with old carbon pools enriched in bomb-C and high respiration rates, which create fluxes that are isotopically distinct from the background atmosphere. These describe the conditions found in mature and old growth forests.

An advantage of the canopy-minus-background approach was that it required measuring canopy $^{14}CO_2$ at only one height, and we applied the method to utilize existing analyses from the NOAA flask network. In the future, however, this approach could be improved by sampling immediately above the forest canopy and using the above-canopy samples for background subtraction. Synchronous sampling between the canopy and background samples would also reduce uncertainty related to changing fossil influences.

Expanding on efforts to observe ^{14}C-R_{eco} in more locations and at more time points would provide valuable information on ^{14}C isotopic disequilibrium, which could be used to improve top-down models of the global terrestrial carbon sink (i.e., based on long-term declines in atmospheric $\Delta^{14}CO_2$). Researchers investigating global radiocarbon budgets presently rely on models to estimate terrestrial ^{14}C disequilibrium, and although the CASA Earth system model showed close agreement to WCR heterotrophic respiration rates, it substantially underestimated the age of heterotrophic respiration.

With refinement of atmospheric sampling techniques, the exciting prospect of using $\Delta^{14}C$ to partition R_{eco} into heterotrophic and autotrophic sources may be possible, because of the large separation of heterotrophic and autotrophic end-members determined through chamber measures. A caveat as discussed by *Phillips et al.* [2013] and shown by *Hopkins et al.* [2013], however, is that autotrophic and heterotrophic soil respiration $\Delta^{14}C$ are dynamic through time. At WCR, the best opportunity for distinguishing heterotrophic and autotrophic end-members is at the end of the growing season, when autotrophic respiration has been most heavily influenced by current year photosynthates and is most similar to atmospheric $\Delta^{14}CO_2$.

Another important potential use of $\Delta^{14}C$-R_{eco} observations is to monitor forest carbon dynamics, and the data presented here can serve as a benchmark from which to monitor future shifts in the sources of respired carbon. Both climate change and disturbances such as logging could be expected to destabilize old soil carbon [*Hopkins et al.*, 2014]. This would lead to an expected increase in $\Delta^{14}C$-R_{eco} at WCR that could be examined in future studies.

References

Andrews, A. E., et al. (2013), CO_2, CO and CH_4 measurements from the NOAA Earth System Research Laboratory's Tall Tower Greenhouse Gas Observing Network: Instrumentation, uncertainty analysis and recommendations for future high-accuracy greenhouse gas monitoring efforts, *Atmos. Meas. Tech.*, *6*, 1461–1553.

Baldocchi, D., and D. R. Bowling (2005), Theoretical examination of Keeling-plot relationships for carbon dioxide in a temperate broadleaved forest with a biophysical model, CANISOTOPE, in *Global Biogeochemical Cycles in the Climate System*, edited by E.-D. Schulze, pp. 109–124, Academic Press, San Diego, Calif.

Bolstad, P. V., K. J. Davis, J. G. Martin, B. D. Cook, and W. Wang (2004), Component and whole-system respiration fluxes in northern deciduous forests, *Tree Physiol.*, *24*, 493–504.

Bowling, D., N. McDowell, B. Bond, B. Law, and J. Ehleringer (2002), ^{13}C content of ecosystem respiration is linked to precipitation and vapor pressure deficit, *Oecologia*, *131*, 113–124.

Bowling, D. R., S. P. Burns, T. J. Conway, R. K. Monson, and J. W. C. White (2005), Extensive observations of CO_2 carbon isotope content in and above a high-elevation subalpine forest, *Global Biogeochem. Cycles*, *19*, GB3023, doi:10.1029/2004GB002394.

Carbone, M. S., C. I. Czimczik, T. F. Keenan, P. F. Murakami, N. Pederson, P. G. Schaberg, X. Xu, and A. D. Richardson (2013), Age, allocation and availability of nonstructural carbon in mature red maple trees, *New Phytol.*, *200*, 1145–1155.

Carvalhais, N., et al. (2014), Global covariation of carbon turnover times with climate in terrestrial ecosystems, *Nature*, *514*, 213–217, doi:10.1038/nature13731.

Cook, B. D., et al. (2004), Carbon exchange and venting anomalies in an upland deciduous forest in northern Wisconsin, USA, *Agric. For. Meteorol.*, *126*, 271–295.

Czimczik, C. I., S. E. Trumbore, M. S. Carbone, and G. C. Winston (2006), Changing sources of soil respiration with time since fire in a boreal forest, *Global Change Biol.*, *12*, 957–971.

Davis, K. J., P. S. Bakwin, C. Yi, B. W. Berger, C. Zhao, R. M. Teclaw, and J. G. Isebrands (2003), The annual cycles of CO_2 and H_2O exchange over a northern mixed forest as observed from a very tall tower, *Global Change Biol.*, *9*, 1278–1293.

DeLucia, E. H., J. E. Drake, R. B. Thomas, and M. Gonzalez-Meler (2007), Forest carbon use efficiency: Is respiration a constant fraction of gross primary production?, *Global Change Biol.*, *13*, 1157–1167.

Desai, A. R., P. V. Bolstad, B. D. Cook, K. J. Davis, and E. V. Carey (2005), Comparing net ecosystem exchange of carbon dioxide between an old-growth and mature forest in the upper Midwest, USA, *Agric. For. Meteorol.*, *128*, 33–55.

Desai, A. R., B. R. Helliker, P. R. Moorcroft, A. E. Andrews, and J. A. Berry (2010), Climatic controls of interannual variability in regional carbon fluxes from top-down and bottom-up perspectives, *J. Geophys. Res.*, *115*, doi:10.1029/2010JG001423.

Ewing, S. A., J. Sanderman, W. T. Baisden, Y. Wang, and R. Amundson (2006), Role of large-scale soil structure in organic carbon turnover: Evidence from California grassland soils, *J. Geophys. Res.*, *111*, G03012, doi:10.1029/2006JG000174.

Friend, A. D., et al. (2014), Carbon residence time dominates uncertainty in terrestrial vegetation responses to future climate and atmospheric CO_2, *Proc. Natl. Acad. Sci. U.S.A.*, *111*, 3280–3285.

Gaudinski, J. B., S. E. Trumbore, E. A. Davidson, and S. Zheng (2000), Soil carbon cycling in a temperate forest: Radiocarbon-based estimates of residence times, sequestration rates and partitioning of fluxes, *Biogeochemistry*, *51*, 33–69.

Gaudinski, J. B., M. S. Torn, W. J. Riley, C. Swanston, S. E. Trumbore, J. D. Joslin, H. Majdi, T. E. Dawson, and P. J. Hanson (2009), Use of stored carbon reserves in growth of temperate tree roots and leaf buds: Analyses using radiocarbon measurements and modeling, *Global Change Biol.*, *15*, 992–1014.

Gaudinski, J. B., M. S. Torn, W. J. Riley, T. E. Dawson, J. D. Joslin, and H. Majdi (2010), Measuring and modeling the spectrum of fine-root turnover times in three forests using isotopes, minirhizotrons, and the Radix model, *Global Biogeochem. Cycles*, *24*, GB3029, doi:10.1029/2009GB003649.

Gloor, M., P. Bawkin, P. P. Tans, D. Hurst, and L. Lock (2001), What is the concentration footprint of a tall tower?, *J. Geophys. Res.*, *106*, 17,831–17,840, doi:10.1029/2001JD900021.

Graven, H. D., T. P. Guilderson, and R. F. Keeling (2007), Methods for high-precision ^{14}C AMS measurement of atmospheric CO_2 at LLNL, *Radiocarbon*, *49*, 349–356.

Graven, H. D., T. P. Guilderson, and R. F. Keeling (2012), Observations of radiocarbon in CO_2 at La Jolla, California, USA 1992–2007: Analysis of the long-term trend, *J. Geophys. Res.*, *117*, D02302, doi:10.1029/2011JD016533.

Hardie, S. M. L., M. H. Garnett, A. E. Fallick, N. J. Ostle, and A. P. Rowland (2009), Bomb-^{14}C analysis of ecosystem respiration reveals that peatland vegetation facilitates release of old carbon, *Geoderma*, *153*, 393–401.

Heckman, K., H. Throckmorton, C. Clingensmith, F. J. González Vila, W. R. Horwath, H. Knicker, and C. Rasmussen (2014), Factors affecting the molecular structure and mean residence time of occluded organics in a lithosequence of soils under ponderosa pine, *Soil Biol. Biochem.*, *77*, 1–11.

Helliker, B. R., J. A. Berry, A. K. Betts, K. J. Davis, J. M. Miller, A. S. Denning, P. S. Bakwin, J. R. Ehleringer, M. P. Butler, and D. M. Ricciuto (2004), Estimates of net CO_2 flux by application of equilibrium boundary layer concepts to CO_2 and water vapor measurements from a tall tower, *J. Geophys. Res.*, *109*, D20106, doi:10.1029/2004JD004532.

Hicks Pries, C. E., E. A. G. Schuur, and K. G. Crummer (2013), Thawing permafrost increases old soil and autotrophic respiration in tundra: Partitioning ecosystem respiration using d^{13}C and D^{14}C, *Global Change Biol.*, *19*, 649–661.

Högberg, P., A. Nordgren, N. Buchmann, A. F. S. Taylor, A. Ekblad, M. N. Högberg, G. Nyberg, M. Ottosson-Löfvenius, and D. J. Read (2001), Large-scale forest girdling shows that current photosynthesis drives soil respiration, *Nature*, *411*, 789–792.

Hopkins, F., M. A. Gonzalez-Meler, C. E. Flower, D. J. Lynch, C. Czimczik, J. Tang, and J.-A. Subke (2013), Ecosystem-level controls on root-rhizosphere respiration, *New Phytol.*, *199*, 339–351.

Hopkins, F., T. R. Filley, G. Gleixner, M. Lange, S. M. Top, and S. E. Trumbore (2014), Increased belowground carbon inputs and warming promote loss of soil organic carbon through complementary microbial responses, *Soil Biol. Biochem.*, *76*, 57–69.

Hua, Q. (2013), Atmospheric radiocarbon for the period 1950–2010, *Radiocarbon*, *55*, 2059–2072.

Keeling, C. D. (1958), The concentration and isotopic abundances of carbon dioxide in rural areas, *Geochim. Cosmochim. Acta*, *13*, 322–334.

Lavoie, M., C. L. Phillips, and D. Risk (2015), A practical approach for uncertainty quantification of high-frequency soil respiration using Forced Diffusion chambers, *J. Geophys. Res. Biogeosci.*, *120*, 128–146, doi:10.1002/2014JG002773.

Lehman, S. J., et al. (2013), Allocation of terrestrial carbon sources using ^{14}CO_2: Methods, measurement, and modeling, *Radiocarbon*, *55*, 1484–1495.

Levin, I., T. Naegler, B. Kromer, M. Diehl, R. J. Francey, A. J. Gomez-Pelaez, L. P. Steele, D. Wagenbach, R. Weller, and D. E. Worthy (2010), Observations and modelling of the global distribution and long-term trend of atmospheric ^{14}CO_2, *Tellus B*, *62*, 26–46.

Lupascu, M., J. M. Welker, U. Seibt, X. Xu, I. Velicogna, D. S. Lindsey, and C. I. Czimczik (2014), The amount and timing of precipitation control the magnitude, seasonality and sources (^{14}C) of ecosystem respiration in a polar semi-desert, northwestern Greenland, *Biogeosciences*, *11*, 4289–4304.

Miller, J., et al. (2013), Initial results of an intercomparison of AMS-based atmospheric [14]CO$_2$ measurements, *Radiocarbon*, *55*, 2–3, doi:10.2458/azu_js_rc.55.16382.

Miller, J. B., and P. P. Tans (2003), Calculating isotopic fractionation from atmospheric measurements at various scales, *Tellus B*, *55*, 207–214.

Miller, J. B., et al. (2012), Linking emissions of fossil fuel CO$_2$ and other anthropogenic trace gases using atmospheric [14]CO$_2$, *J. Geophys. Res.*, *117*, D08302, doi:10.1029/2011JD017048.

Naegler, T., and I. Levin (2006), Closing the global radiocarbon budget 1945–2005, *J. Geophys. Res.*, *111*, D12311, doi:10.1029/2005JD006758.

Neff, J. C., J. C. Finlya, S. A. Zimov, S. P. Davydov, J. J. Carrasco, and E. A. G. Schuur (2006), Seasonal changes in the age and structure of dissolved organic carbon in Siberian rivers and streams, *Geophys. Res. Lett.*, *33*, L23401, doi:10.1029/2006GL028222.

Nickerson, N., J. Egan, and D. Risk (2014), Subsurface approaches for measuring soil CO$_2$ isotopologue flux: Theory and application, *J. Geophys. Res. Biogeosci.*, *119*, 614–629, doi:10.1002/2013JG002508.

Ogée, J., P. Peylin, P. Ciais, T. Bariac, Y. Brunet, P. Berbigier, C. Roche, P. Richard, G. Bardoux, and J.-M. Bonnefond (2003), Partitioning net ecosystem carbon exchange into net assimilation and respiration using [13]CO$_2$ measurements: A cost-effective sampling strategy, *Global Biogeochem. Cycles*, *17*(2), 1070, doi:10.1029/2002GB001995.

Pataki, D. E., J. R. Ehleringer, L. B. Flanagan, D. Yakir, D. R. Bowling, C. J. Still, N. Buchmann, J. O. Kaplan, and J. A. Berry (2003), The application and interpretation of Keeling plots in terrestrial carbon cycle research, *Global Biogeochem. Cycles*, *17*(1), 1022, doi:10.1029/2001GB001850.

Phillips, C. L., K. J. McFarlane, D. Risk, and A. R. Desai (2013), Biological and physical influences on soil [14]CO$_2$ seasonal dynamics in a temperate hardwood forest, *Biogeosciences*, *10*, 7999–8012.

Randerson, J. T., I. G. Enting, E. A. G. Schuur, K. Caldeira, and I. Y. Fung (2002), Seasonal and latitudinal variability of troposphere Δ[14]CO$_2$: Post bomb contributions from fossil fuels, oceans, the stratosphere, and the terrestrial biosphere, *Global Biogeochem. Cycles*, *16*(4), 1112, doi:10.1029/2002GB001876.

Raupach, M. R. (2001), Inferring biogeochemical sources and sinks from atmospheric concentrations: General considerations and applications in vegetation canopies, in *Global Biogeochemical Cycles in the Climate System*, edited by E.-D. Schulze, pp. 41–59, Academic Press, San Diego, Calif.

Rey, A., G. Etiope, L. Belelli-Marchesini, D. Papale, and R. Valentini (2012), Geologic carbon sources may confound ecosystem carbon balance estimates: Evidence from a semiarid steppe in the southeast of Spain, *J. Geophys. Res.*, *117*, G03034, doi:10.1029/2012JG001991.

Richardson, A. D., M. S. Carbone, T. F. Keenan, C. I. Czimczik, D. Y. Hollinger, P. Murakami, P. G. Schaberg, and X. Xu (2013), Seasonal dynamics and age of stemwood nonstructural carbohydrates in temperate forest trees, *New Phytol.*, *197*, 850–861.

Risk, D., N. Nickerson, C. Creelman, G. McArthur, and J. Owens (2011), Forced diffusion soil flux: A new technique for continuous monitoring of soil gas efflux, *Agric. For. Meteorol.*, *151*, 1622–1631.

Schlesinger, W. H., and J. A. Andrews (2000), Soil respiration and the global carbon cycle, *Biogeochemistry*, *48*, 7–20.

Schmidt, M. W. I., et al. (2011), Persistence of soil organic matter as an ecosystem property, *Nature*, *478*, 49–56.

Schuur, E. A. G., and S. E. Trumbore (2006), Partitioning sources of soil respiration in boreal spruce forest using radiocarbon, *Global Change Biol.*, *12*, 165–176, doi:10.1111/j.1365-2486.2005.01066.x.

Schuur, E. A. G., S. E. Trumbore, M. C. Mack, and J. W. Harden (2003), Isotopic composition of carbon dioxide from a boreal forest fire: Inferring carbon loss from measurements and modeling, *Global Biogeochem. Cycles*, *17*, 1001, doi:10.1029/2001GB001840.

Stuiver, M., and H. A. Polach (1977), Discussion: Reporting of ^{14}C data, *Radiocarbon*, *19*, 355–363.

Thomas, C. K., J. G. Martin, B. E. Law, and K. Davis (2013), Toward biologically meaningful net carbon exchange estimates for tall, dense canopies: Multi-level eddy covariance observations and canopy coupling regimes in a mature Douglas-fir forest in Oregon, *Agric. For. Meteorol.*, *173*, 14–27.

Thompson, M. V., and J. T. Randerson (1999), Impulse response functions of terrestrial carbon cycle models: Method and application, *Global Change Biol.*, *5*, 371–394.

Torn, M. S., S. E. Trumbore, O. A. Chadwick, P. M. Vitousek, and D. M. Hendricks (1996), Mineral control of soil organic carbon storage and turnover, *Nature*, *389*, 170–173.

Trumbore, S. E. (2000), Age of soil organic matter and soil respiration: Radiocarbon constraints on belowground C dynamics, *Ecol. Appl.*, *10*, 399–411.

Trumbore, S. E. (2009), Radiocarbon and soil carbon dynamics, *Annu. Rev. Earth Planet. Sci.*, *37*, 47–66.

Tu, K., and T. E. Dawson (2005), Partitioning ecosystem respiration using stable carbon isotope analyses of CO$_2$, in *Global Biogeochemical Cycles in the Climate System*, edited by E.-D. Schulze, pp. 125–153, Academic Press, San Diego, Calif.

Turnbull, J., P. Rayner, J. Miller, T. Naegler, P. Ciais, and A. Cozic (2009), On the use of [14]CO$_2$ as a tracer for fossil fuel CO$_2$: Quantifying uncertainties using an atmospheric transport model, *J. Geophys. Res.*, *114*, D22302, doi:10.1029/2009JD012308.

Van Gorsel, E., et al. (2009), Estimating nocturnal ecosystem respiration from the vertical turbulent flux and change in storage of CO$_2$, *Agric. For. Meteorol.*, *149*, 1919–1930.

Vasys, V. N., A. R. Desai, G. A. McKinley, V. Bennington, A. M. Michalak, and A. E. Andrews (2011), The influence of carbon exchange of a large lake on regional tracer-transport inversions: Results from Lake Superior, *Environ. Res. Lett.*, *6*, 034016.

Vaughn, B. H., J. B. Miller, D. F. Ferretti, and J. C. White (2004), Stable isotope measurements of atmospheric CO$_2$ and CH$_4$, in *Handbook of Stable Isotope Analytical Techniques*, edited by P. de Groot, pp. 272–304, Elsevier Academic Press, San Diego, Calif.

Zobitz, J. M., J. P. Keener, H. Schnyder, and D. R. Bowling (2006), Sensitivity analysis and quantification of uncertainty for isotopic mixing relationships in carbon cycle research, *Agric. For. Meteorol.*, *136*, 56–75.